THE INDEPENDENT AND COMBINED EFFECTS OF RAPAMYCIN AND METFORMIN ON NATURALLY OCCURRING OSTEOARTHRITIS

BY

DENNIS MICHAEL MINTON

THESIS

Submitted in partial fulfillment of the requirements
for the degree of Master of Science in Kinesiology
in the Graduate College of the
University of Illinois at Urbana-Champaign, 2020

Urbana, Illinois

Adviser:

Assistant Professor Adam Konopka

ABSTRACT

Osteoarthritis (OA) is among the top 10 diseases limiting human healthspan, and no disease modifying therapies currently exist. OA is a degenerative disease of the whole joint, characterized by articular cartilage loss, subchondral bone sclerosis, meniscal calcification, synovitis, and skeletal muscle dysfunction. Inhibiting the mechanistic target of rapamycin (mTOR) and stimulating AMP-activated protein kinase (AMPK) has extended lifespan and protected against post-traumatic (secondary) OA in mice. However, it remains unknown if manipulation of these pathways can protect against naturally occurring, age-related (primary) OA, the form most commonly observed in humans. The outbred Dunkin-Hartley (DH) guinea pig develops primary OA beginning at 5 months of age and displays high histological similarity to human OA. Therefore, at 5 months we sacrificed a group of DH guinea pigs to serve as young control and the remaining animals were randomized to receive a standard diet (age-matched controls) or diets enriched with rapamycin (Rap; 14ppm), metformin (Met; 1000ppm), or a combination of rapamycin plus metformin (Rap+Met) for 3 months. Hind limbs were collected for histopathological and radiographic evaluation of the knee joint. Histological OA scores in DH guinea pigs receiving Rap and Rap+Met were significantly lower than their age-matched controls. Rap treatment also reduced subchondral cortical bone thickness in the medial and lateral tibia, while Rap+Met reduced cortical thickness only in the lateral tibia. Both OA scores and cortical thickness were highly correlated with bodyweight, suggesting reduced joint loading could be contributing to the protective effects of Rap and Rap+Met. The minimal effect of Met may be attributed to low dose and indicates that Rap likely drove the protective effects of Rap+Met. Together, these data are the first to suggest that mTOR inhibition delays the onset of primary, age-related OA in the DH guinea pig.

TABLE OF CONTENTS

CHAPTER 1: INTRODUCTION

Osteoarthritis (OA) is a common joint disorder affecting older adults and is among the top 10 diseases limiting human healthspan and lifespan (Murray et al., 2013). OA is a disease of the whole joint, characterized by articular cartilage degeneration, thickening of subchondral bone, osteophyte formation, synovitis, meniscal calcification, and skeletal muscle dysfunction (R. F. Loeser, Goldring, Scanzello, & Goldring, 2012). Advanced age is the single greatest risk factor for developing OA with prevalence reaching up to 75% of adults over 70 years (Neogi & Zhang, 2013). With no disease modifying therapies available for OA, treatment is limited to symptom management and eventually total joint replacement. Therefore, as the already large aged population continues to grow, the $140 billion annual OA-associated medical costs are expected to inflate (Murphy, Cisternas, Pasta, Helmick, & Yelin, 2018).

During OA progression, chondrocytes, the only resident cell type in articular cartilage, undergo a hallmark homeostatic shift towards catabolism, driven by increased expression of proteolytic enzymes accompanied by negligible upregulation in associated inhibitors (Woessner & Gunja-Smith, 1991). Proteoglycan is the primary structural protein in hyaline cartilage and is responsible for its natural resistance to compressive load. Due to this catabolic shift, the abundance of proteoglycan is markedly reduced, rendering the cartilage less equipped to resist the stresses of joint loading (Stockwell, 1991). Underneath, in the subchondral bone, development of sclerotic lesions and heterogeneous stiffness distribution can expose cartilage to shear and tensile stresses, further increasing risk for fibrillation and failure (Burr & Gallant, 2012; E. L. Radin & Rose, 1986).

Within the joint space, the menisci assist in facilitating the load from the femoral condyles to the tibial plateaus and ensuring smooth articulation. These cartilage formations are the site of

progressive calcium phosphate crystal deposition, which ossifies the menisci and disables their normal load diffusing function (Sun & Mauerhan, 2012). The degree of pathological ossification of the menisci closely mirrors histological OA severity in the affected compartment and clinical symptoms (Fuerst et al., 2009). These factors, coupled with chronic synovitis and inflammation, osteophyte formation, and reduction of periarticular muscle quality, lead to pain, reduced joint mobility, and loss of function (R. F. Loeser et al., 2012). While increased protease expression and some altered biomechanical factors are well characterized, the underlying signaling disruptions catalyzing OA pathology are not fully understood.

OA can manifest in two forms. Post-traumatic (secondary) OA develops in response to injury and non-traumatic, age-related (primary) OA develops naturally over time. It has been estimated that primary OA accounts for as many as 91% of all cases in humans (T. D. Brown, Johnston, Saltzman, Marsh, & Buckwalter, 2006). However, it is difficult to predict and study the early onset and progression of primary OA in humans because of its idiopathic and insidious nature. To circumvent this issue, preclinical research typically employs injury-induced models of OA in mice. While this is time and cost effective, there is a growing body of evidence to suggest that, although primary and secondary OA share similar pathological outcomes, they are driven by distinct mechanisms. Only 10% of differentially upregulated and 35% of differentially downregulated genes are conserved between primary and secondary OA (Aki, Hashimoto, Ogasawara, & Itoi, 2018). There have also been several reports of genes playing inconsistent or opposing roles in primary and secondary OA. Deletion of *Panx3*, while protective against injury-induced OA, has a detrimental effect on age-related OA pathology (Moon, Shao, Penuela, Laird, & Beier, 2018). While, to our knowledge, this is the most extreme dichotomy between genes differentially involved in primary and secondary OA, deletion of *Mink1* (Yu et al., 2020), *JNK1*

and *JNK2* (R. Loeser, Kelley, Harper, & Carlson, 2018), *Atg5* (Bouderlique et al., 2016), *Trpv4* (O'Conor et al., 2016), and *Tgfα* (Usmani et al., 2016) all exert contrasting effects on primary and secondary OA. Together, these studies support the idea that unique mechanisms underpin primary and secondary OA and highlight the need to investigate therapeutic targets in both OA subtypes.

There is an intimate link between several biological hallmarks driving both aging and the onset of age-related chronic disease (Kennedy et al., 2014). The mechanistic target of rapamycin (mTOR) and AMP-activated protein kinase (AMPK) are two energy sensing pathways similarly dysregulated during aging and chronic diseases such as OA (Johnson, Rabinovich, & Kaeberlin, 2013; Pal, Endisha, Zhang, & Kapoor, 2015; Salminen & Kaarniranta, 2012; Zhou et al., 2017). mTOR is an evolutionarily conserved kinase which serves as a regulator of cellular metabolism including proliferation, protein synthesis, senescence, and survival (Loewith & Hall, 2011). Constitutively active mTOR during adulthood stimulates aberrant cellular proliferation at the cost of cell maintenance and stress resistance (Demidenko & Blagosklonny, 2008). AMPK is a highly conserved regulator of cellular energy homeostasis that exerts a myriad of effects thought to be beneficial for aging, including stimulation of autophagy (Hardie, Ross, & Hawley, 2012). Rapamycin bound to FKBP12 directly binds and inhibits mTOR (Sabers et al., 1995), and the commonly prescribed anti-diabetic drug metformin is proposed to stimulate AMPK both directly (Hawley, Gadalla, Olsen, & Hardie, 2002) and indirectly through mild inhibition of mitochondrial complex I (Owen, Doran, & Halestrap, 2000). Rapamycin extends median and maximal lifespan in multiple species while metformin treatment increases lifespan in some but not all studies (Jie Chen et al., 2017; Harrison et al., 2009; Kaeberlein et al., 2005; Martin-Montalvo et al., 2013; Strong et al., 2016; Vellai et al., 2003). However, extending lifespan without delaying the onset or slowing the progression of debilitating age-associated conditions could be viewed as detrimental.

Therefore, it is imperative to understand if targeting the fundamental biology of aging could be a successful strategy to delay the onset of naturally occurring, primary OA.

In articular cartilage, mTOR activity increases with age in mice and activation of mTOR by cartilage-specific knockout of tuberous sclerosis complex 1 (TSC1), an upstream inhibitor of mTOR, initiates OA pathology in young, male mice (H. Zhang et al., 2017). Recent evidence indicates that cartilage-specific knockout (Y. Zhang et al., 2015) and pharmacological inhibition of mTOR (Caramés et al., 2012; Takayama et al., 2014) decreases OA pathology secondary to injury in young, male mice and rabbits. While these studies build support for mTOR-based therapeutics for the treatment of OA, the completed studies were in injury-induced models of OA. To our knowledge, no studies have examined the role of mTOR inhibition in delaying the onset of naturally occurring OA, the most common form of OA observed clinically in older adults.

In healthy cartilage, AMPK signaling preserves chondrocyte homeostasis and extracellular matrix integrity by resisting inflammatory stressors (Bohensky, Leshinsky, Srinivas, & Shapiro, 2010; Terkeltaub, Yang, Lotz, & Liu-Bryan, 2011). Loss of AMPK activity occurs with age (Reznick et al., 2007) and results in increased protease expression, blunted matrix anabolic response, and apoptosis in human chondrocytes, and contributes to more severe OA pathology in male mice (Petursson et al., 2013; Terkeltaub et al., 2011; Zhou et al., 2017). Metformin and other AMPK-activators have chondroprotective effects against inflammatory induced protease expression *in vitro* (Petursson et al., 2013; C. Wang et al., 2018) and protect against injury-induced OA in young male mice (Feng et al., 2020; Li et al., 2020) and rhesus monkeys (Li et al., 2020). In obese patients with OA, metformin use is associated with a lower rate of medial cartilage volume loss and decreased risk of total knee replacement (Y. Wang et al., 2019). However, the role of AMPK activity has not yet been investigated prospectively in primary OA.

While mouse models of OA are valuable for mechanistic discovery, their translation to humans is limited. Mice have distinct cartilage anatomy compared to humans, and injury-induced OA does not fully recapitulate the primary OA most commonly seen in humans (Glasson, Chambers, Van Den Berg, & Little, 2010). To circumvent these limitations, the Dunkin-Hartley (DH) guinea pig is a well-characterized outbred model of primary OA that predictably develops OA pathology as early as 3 months of age (A. M. Bendele & Hulman, 1988). OA disease progression in the DH guinea pig displays a high degree of histopathological similarity to the human condition (Kraus, Huebner, DeGroot, & Bendele, 2010). Articular cartilage degeneration, osteophytosis, subchondral sclerosis, and ossification of the menisci in the DH guinea pig are age-related and share a similar spatial progression to humans (Huebner & Kraus, 2006; Kapadia et al., 2000). Collectively, these characteristics support the use of the DH guinea pig to study the mechanisms involved in the initiation and treatment of primary OA.

The purpose of this study was to determine if dietary rapamycin, metformin, or a combination of rapamycin plus metformin treatment can delay the onset or slow the progression of primary OA in DH guinea pigs. We hypothesized that 3 months of rapamycin, metformin and rapamycin+metformin started at 5 months of age would lower histological knee OA severity in DH guinea pigs. This study provides a unique contribution as it is the first to evaluate if lifespan extending treatments that slow the biological rate of aging can modify primary OA, the most prevalent form of OA observed in older adults.

CHAPTER 2: METHODOLOGY

2.1 ANIMAL USE

All animal procedures were approved by the Institutional Animal Care and Use Committee at the University of Illinois at Urbana-Champaign. Male, Dunkin-Hartley guinea pigs were obtained from Charles River in two cohorts of 18 and 17 animals. Animals were singly housed in 30.8x59.4x22.9 cm clear plastic, flat bottomed cages (Thoren, Model #6) with bedding. 12 hour light/dark cycles were used beginning at 0600. DH Guinea pigs were allowed to acclimate for 2-3 weeks before study measurements were collected. DH Guinea pigs were provided water and a standard chow diet (Evigo 2040) fortified with vitamin C (1050 ppm) and Vitamin D (1.5 IU/kg) ad libitum until 5 months of age. DH Guinea pigs were then either sacrificed to serve as young, non-OA controls (n=3), or continued the control diet (n=8), or diets enriched with encapsulated rapamycin (14 ppm, n=8), metformin (1000 ppm, n=8), or the combination of encapsulated rapamycin+metformin (14 ppm, 1000 ppm, n=8) as outlined in Figure 1. DH Guinea pigs were randomized to match bodyweight between groups prior to beginning treatment. Diets were manufactured by Envigo and enriched at concentrations previously used by the NIH Interventions Testing Program (Miller et al., 2014; Strong et al., 2016). Microencapsulated Rapamycin (Rapamycin holdings) allows increased survival of the compound during diet preparation and prevents digestion in the stomach (Nadon et al., 2008). Metformin was obtained from AK Scientific (I506). Guinea pigs began their experimental diet at ~5 months of age for 3 months. Food consumption was recorded on Monday, Wednesday, and Friday between 8 and 9 AM, and body weight was recorded before feeding on Monday. Guinea pigs provided experimental diets enriched with rapamycin, metformin or the combination of rapamycin + metformin were allowed

continued ad libitum access to food and water. Previous studies have shown that dietary Rap treatment, at the same dose provided in our study, significantly reduced bodyweight in male (Miller et al., 2011, 2014; Weiss, Fernandez, Liu, Strong, & Salmon, 2018) and female (Miller et al., 2011; Weiss et al., 2018) mice. Therefore, we restricted food consumption in the control group to match the food consumption of the experimental diet to minimize the influence of food intake on dependent variables.

2.2 ANALYSIS OF RAPAMYCIN AND METFORMIN IN DIET AND BLOOD

To ensure scientific rigor, samples of diets enriched with rapamycin, metformin or the combination of rapamycin+metformin, and aliquots of whole blood (collected as described later) were sent to the Bioanalytical Pharmacology Core at the San Antonio Nathan Shock Center to confirm drug concentrations in the diet and in circulation. Analysis was performed using tandem HPLC-MS as described elsewhere (Harrison et al., 2009; Tardif et al., 2015).

2.3 TISSUE COLLECTION

Following 3 months of treatment, two animals were sacrificed daily between 7 AM and 11 AM. Food and water were removed from the cages 2-4 hours before euthanasia. Animals were anesthetized in a chamber containing 5% isoflurane gas in oxygen and maintained using a gas mask with 1.5-3% isoflurane. Once reflexively unresponsive, the thoracic cavity was opened for blood collection by cardiac venipuncture and subsequent excision of the heart. After death, the right hind limb was removed at the coxofemoral joint and fixed in 10% neutral buffered formalin for 48 hours, then transferred to 70% ethanol for storage until processed for histology. The soleus

muscle was also collected from the left hind limb, snap frozen in liquid nitrogen, and stored at -80C for further analysis.

2.4 HISTOLOGY

Knee joints were decalcified in a 5% EDTA solution, changed every 2-3 days, for 6 weeks. Joints were then cut in a coronal plane along the axis of the medial collateral ligament as described (Kraus et al., 2010). The transected joint was embedded in paraffin and sectioned at 5 micrometer increments, stained with Toluidine Blue as recommended by the Osteoarthritis Research Society International (OARSI) guidelines (Kraus et al., 2010). Slides were scanned using the Hamamatsu NanoZoomer Digital Pathology System, providing 460 nm resolution. Scan focus points were set manually along the articular cartilage. Imaged slides were then scored in a blinded fashion for OA severity as described by the OARSI Modified Mankin guidelines (Kraus et al., 2010).

2.5 ISOLATION AND CULTURE OF PRIMARY PORCINE CHONDROCYTES

Healthy cartilage was scraped from porcine metacarpophalangeal joints and chondrocytes were isolated by enzymatic digestion using pronase (Sigma, 11459643001) and type II collagenase (Worthington Medical, LS004176). Chondrocytes were then seeded at a density of $5x10^5$ cells/well in 6-well plates and resuspended in Dulbecco's modified Eagle's medium (DMEM) containing 4.5 g/L glucose, HEPES buffer, and L-glutamine (Fisher, 12430062). Media was supplemented with 5% fetal bovine serum (FBS), 100x non-essential amino acids, and antibiotics (100 U/mL penicillin and 0.1 mg/mL streptomycin). Cells were cultured for 4 days at 37°C and 5% CO_2 until confluency was reached at which point they were treated with rapamycin at 0.5, 1, 1.5, 2, or 3 nM

for 48 hours. Cells were then washed once in PBS without Ca^{2+} or Mg^{2+} before being collected in 250 uL of RIPA buffer and flash frozen in liquid N_2.

2.6 TISSUE HOMOGENIZATION AND WESTERN BLOT ANALYSIS

Cells were lysed and homogenized by sonication, and soleus muscles were pulverized using a liquid nitrogen-cooled mortar and pestle. 50 mg of soleus homogenate was then suspended in 1mL of RIPA buffer with freshly added Halt™ protease and phosphatase inhibitor cocktail (ThermoFisher, 78430) and 60 mg of zirconium oxide beads. Supernatant was collected following two 3-minute cycles in a Bullet Blender bead homogenizer (Next Advance) and microcentrifugation at 800g. Samples were diluted to equal concentrations following a bicinchoninic acid (BCA) assay (ThermoFisher, 23225) to determine total protein concentration. Protein denaturation was achieved using Laemmli Sample Buffer (Bio-Rad, 1610737) with 2-mercaptoethanol (Bio-Rad, 1610710) and heating for 5 minutes at 95°C.

Twenty micrograms of protein were loaded per lane for sodium-dodecyl-sulfate polyacrylamide-gel-electrophoresis (SDS-PAGE) using a 4-15% Mini PROTEAN gradient gel (Bio-Rad, 4561083). Protein was transferred to polyvinylidene fluoride (PVDF) membranes and blocked for 1 hour at room temperature using 5% bovine serum albumin (BSA) in Tris-buffered saline with 0.1% Tween-20 (TBST). Membranes were then incubated with rabbit monoclonal antibodies raised against ribosomal protein S6 (rpS6; 1:1,000 in 5% BSA/TBST; Cell Signaling 2217) and rpS6 phosphorylated at Ser235/236 (p-rpS6; 1:2,000 in 5% BSA/TBST; Cell Signaling, 4858) overnight at 4°C. After three 5-minute TBST washes, membranes were incubated with a horseradish peroxidase (HRP)-linked anti-rabbit IgG (1:10,000 in 5% BSA/TBST; Cell Signaling 7074) for 1 hour at room temperature. Membranes the underwent three 5-minute TBST washes

followed by an incubation in SuperSignal West Dura Extended Duration Substrate (ThermoFisher 34076) and were imaged using a ChemiDoc XRS+System (Bio-Rad 1708265). Protein bands were quantified by densitometry using the Quantity One imaging program and were expressed as a ratio of phosphorylated- to total rpS6.

2.7 MICRO COMPUTED TOMOGRAPHY (μCT)

Right hind limbs were scanned using a Rigaku CT Lab GX130 at 120 uA and 110 kV for 14 minutes, achieving a pixel size of 49 um. Half of the guinea pigs (n=4 per group) were scanned. All scans were segmented using identical thresholds to allow comparison between animals. Scans were first processed in Amira 6.7 (ThermoFisher) to create 3D joint reconstructions. Ossified meniscus volume was quantified using material statistics after segmenting menisci to a separate material. The thickness mapping function was visualized using a temperature-based volume rendering to illustrate spatial thickness distribution across the subchondral plates. A series of dilation, erosion, filling, and image subtraction functions were then used to isolate trabecular and cortical bone similar to the method described (Buie, Campbell, Klinck, MacNeil, & Boyd, 2007). Scans were resliced 4 times along axes perpendicular to medial and lateral tibial and femoral articular surfaces and binarized.

NIH ImageJ software and BoneJ plugin were used to quantify thickness, spacing, and volume fraction measurements (Doube et al., 2010; Schneider, Rasband, & Eliceiri, 2012). Regions of interest (ROI) were placed along the articular surfaces of the tibial plateaus and femoral condyles to measure subchondral cortical thickness. ROIs were placed in the trabecular bone of the medial and lateral tibia and femur where trabecular thickness, spacing, and bone volume fraction were measured.

2.8 STATISTICAL ANALYSIS

A two-way repeated measures ANOVA (time x treatment) was performed to determine differences in food consumption and body weight. Upon a significant interaction, a Holm-Sidak multiple comparisons test was used. For all other variables, differences were detected using one-way ANOVA with Fisher's Least Significant Difference test comparing treatment groups to 8 month controls. Pearson's R was used to determine correlation between variables. Statistical significance was set a priori at $P<0.05$. Data are presented as mean ± standard error of the mean (SEM).

CHAPTER 3: RESULTS

3.1 INFLUENCE OF RAPAMYCIN, METFORMIN, AND RAPAMYCIN+METFORMIN ON FOOD CONSUMPTION AND BODYWEIGHT

Male DH guinea pigs were provided standard chow or standard chow enriched with rapamycin (Rap), metformin (Met), or rapamycin plus metformin (Rap+Met) for 12 weeks (Figure 2A). The average daily intake of Rap and Met in each diet group is reported in Table 1. There was a main effect for time that was driven by decreased food consumption in the early weeks in DH guinea pigs treated with Rap (Weeks 1 and 2; $p<0.05$), Met (Week 3; $p<0.05$), and Rap+Met (week 1; $p<0.05$). Food consumption did not differ from week 0 the remainder of the study. There were no significant differences between treatments.

Despite largely matching food intake over the 12-week intervention, there was a significant effect of time, treatment and interaction (time by treatment) in body weight. Rap+Met and Rap treated DH guinea pigs were smaller ($p<0.05$) than control starting at week 3 and week 4, respectively, until the end of the study (Figure 2B). There were no differences in body weight between DH guinea pigs treated with Met versus control.

3.2 IMPACT OF RAPAMYCIN, METFORMIN, AND RAPAMYCIN+METFORMIN ON GLUCOSE AND LACTATE METABOLISM

At sacrifice, Rap and Rap+Met treated DH guinea pigs displayed increased blood glucose concentrations compared to control ($p<0.05$; Figure 2C). Lactate concentrations were increased in the Rap+Met group ($p<0.05$; Figure 2D). Treatment with Met alone exerted no apparent effects on

blood glucose or lactate compared to control. Analysis of blood revealed that the experimental diets were sufficient to increase circulating levels of Rap and Met (Figures 2E-F).

3.3 RAPAMYCIN INHIBITED mTOR IN SKELETAL MUSCLE AND PRIMARY PROCINE CHONDROCYTES

Activation of the Ser/Thr kinase mTOR results in a phosphorylation cascade through p70 S6 kinase 1 and its substrate ribosomal protein S6 (rpS6). Therefore, phosphorylation status of rpS6 is commonly used as a surrogate measurement for mTOR activity. To show that Rap is capable of inhibiting mTOR in chondrocytes, the resident cell type in articular cartilage, we cultured primary porcine chondrocytes in media enriched with increasing concentrations of Rap. Phosphorylation of rpS6 was reduced by Rap in a dose-dependent manner, with complete loss of rpS6 phosphorylation at 3 nM (Figure 3A). Western blot analysis of skeletal muscle lysate from the soleus of DH guinea pigs revealed that treatment with Rap and Rap+Met significantly reduced phosphorylation of rpS6 at residues Ser235/236 (Figures 3B-C).

3.4 RAPAMYCIN AND RAPAMYCIN PLUS METFORMIN TREATMENT ATTENUATED THE AGE-RELATED PROGRESSION OF PRIMARY OA IN THE MEDIAL TIBIA

Control animals were sacrificed at 5 and 8 months, which is consistent with the age-related progression of mild to moderate OA in DH guinea pigs. As expected, average OARSI scores (Figure 4B) significantly increased from 5 to 8 months ($p<0.05$), driven by loss of normal chondrocyte cellularity ($p<0.05$; Figure 4C), proteoglycan content ($p<0.05$; Figure 4D), and a non-significant increase in articular cartilage structural damage (ACS; $p=0.11$; Figure 4E). Rap and Rap+Met treatment prevented the progression of age-related OA from 5 to 8 months, as evident by lower total OARSI scores compared to 8-month controls ($p<0.01$; Figure 4E). The protective

effects of Rap were driven primarily by maintained proteoglycan content ($p<0.001$; Figure 4D). There were also trends for Rap to decrease in cellularity disruption ($p=0.05$; Figure 4C) and ACS ($p=0.05$; Figure 4E). Rap+Met prevented the loss of normal cellularity ($p<0.05$; Figure 4C) and proteoglycan content ($p<0.001$; Figure 4D), and ACS ($p=0.05$; Figure 4E). While Met did not decrease the total OA score (Figure 4B), it did maintain proteoglycan content ($p<0.05$; Figure 4D).

3.5 DECREASED SUBCHONDRAL AND DIAPHYSEAL CORTICAL BONE THICKNESS IN RAPAMYCIN TREATED ANIMALS

Mean subchondral cortical thickness was significantly decreased by Rap in the medial ($p<0.05$; Figure 5A) and lateral ($p<0.05$; Figure 5B) tibial plateaus, and non-significantly in the medial femoral condyle ($p=0.06$; Figure 4C). Rap+Met decreased cortical thickness only in the lateral tibia ($p<0.05$; Figure 5B). Met treatment alone exerted no apparent effects on subchondral bone. Further investigation revealed that cortical thickness at the femoral diaphysis was also decreased by Rap ($p<0.001$; Figure 5D) and Rap+Met ($p<0.05$; Figure 5D), and this change was proportionate to the decrease in cortical thickness in articular bone (Figure 5E). Femoral epicondylar width (Figure 5F) was not different between groups, suggesting that our treatments did not affect skeletal development or overall bone architecture.

3.6 BODYWEIGHT CORRELATED WITH REDUCTIONS IN OARSI SCORES AND SUBCHONDRAL THICKNESS

OA scores ($R^2=0.685$, $p=0.0001$; Figure 5A) and medial tibial subchondral thickness ($R^2=0.55$, $p=0.001$; Figure 5B) displayed a significant positive correlation to bodyweight These

data suggest that decreases in OARSI scores and subchondral cortical thickness were associated with Rap and Rap+Met-induced reduction in bodyweight.

CHAPTER 4: DISCUSSION

The purpose of this study was to test if dietary Rap (14ppm), Met (1000ppm) or Rap+Met treatment at concentrations previously shown to extend lifespan can delay the onset of age-related OA in the outbred DH guinea pig. Dietary Rap and Rap+Met treatment prevented the age-related progression of OA severity from 5 to 8 months as evident by lower OARSI scores in articular cartilage from the medial tibial plateau. Rap and Rap+Met also reduced subchondral bone thickness in multiple joint compartments. Changes in OA score and subchondral thickness were correlated with bodyweight, suggesting the protective effects of Rap and Rap+Met may be associated with lower joint loading. Met alone demonstrated little effect on primary OA pathology in articular cartilage or subchondral bone. While Rap and Rap+Met treatment were beneficial for articular cartilage, we did observe off-target effects such as elevated blood glucose and lactate concentrations. Although the mTOR pathway has been investigated in injury-induced models of OA, this is the first study to indicate that mTOR could be a therapeutic target for age-related, primary OA.

Articular cartilage is the hallmark tissue involved in OA pathology and has traditionally been the primary focus of OA research. In our study, Rap and Rap+Met treatment lowered OA scores in the medial tibia of 8-month DH guinea pigs. The dose of Rap consumed in the diet was 0.72±0.06 mg/kg/day and 0.68±0.09 mg/kg/day in the Rap and Rap+Met groups, respectively. This dietary dose of Rap is similar to doses that are protective against secondary OA administered systemically by intra-peritoneal injection (Caramés et al., 2012; 1 mg/kg/day) and locally by intra-articular injection (Takayama et al., 2014; 0.914 mg/kg/day). Additionally, the effect of Rap and Rap+Met on OA pathology in the DH guinea pig resembles the robust protection against secondary

OA in mice by genetic ablation of mTOR (Y. Zhang et al., 2015). This suggests that the protective effects of Rap against OA pathology are driven primarily by its actions within articular cartilage and not off-target effects on other tissues. Additionally, at doses sufficient to extend lifespan and protect against post-traumatic OA in mice, Rap and Rap+Met were shown for the first time to delay the onset of primary, age-related OA pathology in the DH guinea pig.

We also demonstrated that Rap inhibited mTOR in cultured chondrocytes derived from porcine articular cartilage as well as periarticular skeletal muscle in DH guinea pigs, congruent with the effect of Rap on multiple tissues and cell types (N. F. Brown, Stefanovic-Racic, Sipula, & Perdomo, 2007; Caramés et al., 2012; Houde et al., 2010; Philp et al., 2015; Roh, Han, Tzatsos, & Kandror, 2003; Sasaki et al., 2012; C. A. Wolff et al., 2020). In addition to maintaining articular cartilage score and proteoglycan content, Rap+Met maintained normal chondrocyte cellularity in the medial tibial plateau. An increase in cellularity and chondrocyte clustering near articular cartilage damage and fibrillations is thought to be indicative of chondrocyte proliferation and a failed attempt to repair cartilage damage (Rothwell & Bentley, 1973). Activation of mTOR has been shown to initiate the onset of structural OA pathology by stimulating chondrocyte proliferation, and inhibition of cellular proliferation by Rap protected against secondary-OA (H. Zhang et al., 2017). Our unpublished data in cultured chondrocytes suggest that mTOR inhibition by Rap and Rap+Met shifts the allocation of proteostatic resources from cell proliferation to cell maintenance by inhibiting chondrocyte proliferation and maintaining protein synthesis. These findings in culture are consistent with the decrease in cellularity, proteoglycan loss and articular damage in vivo in the DH guinea pigs and likely suggest that Rap and Rap+Met lower OA pathology by restoring proteostatic mechanisms. However, this supposition requires additional

studies to understand how mTOR inhibition effects proteostasis to delay the onset of OA pathology in vivo.

OA progression is characterized by subchondral bone sclerosis, which correlates with articular cartilage loss in humans (Crema et al., 2014) and precedes cartilage damage in some animal models of OA including the DH guinea pig (Burr & Gallant, 2012; Carlson, Loeser, Purser, Gardin, & Jerome, 2009; Huebner, Hanes, Beekman, TeKoppele, & Kraus, 2002; T. Wang, Wen, Yan, Lu, & Chiu, 2013). uCT analysis revealed that treatment with Rap decreased subchondral cortical thickness in the medial and lateral tibia, and Rap+Met decreased thickness in the lateral tibia. Initially, this may be viewed as resistance to sclerotic lesions. Femoral epicondylar width, a joint dimension previously used to assess treatment effects on longitudinal bone growth (Hamrick, Ding, Ponnala, Ferrari, & Isales, 2008), was unchanged between groups. This suggests that Rap treatment prevented subchondral bone sclerosis without influencing the structural development of bone. However, further investigation revealed that changes in subchondral bone thickness were not site-specific and were also observed proportionately at the femoral diaphysis. DH guinea pigs have been reported to reach skeletal maturity between 4 months (Radakovich, Marolf, Culver, & Santangelo, 2019) and 7 months (Kraus et al., 2010; Zuck, 1938). Since Rap and/or Met treatment started at 5 months of age, it is possible that treatment began before skeletal maturity was reached. In support of this idea, DH guinea pigs continue gaining weight until at least 18 months of age (Alison M. Bendele & Hulman, 1991) and during this time there is an increase in tibial and femoral cortical thickness (Radakovich et al., 2018). Therefore, administration of Rap may have halted the rate of bone remodeling and prevented increases in cortical thickness seen in response to normal growth.

The effects of Rap and Rap+Met on cortical thickness are likely due to the effect of mTOR inhibition on skeletal remodeling and development (Jianquan Chen & Long, 2018). Bone remodeling is a dynamic process mediated by osteoblasts and osteoclasts, the cell types responsible for synthesizing and resorbing mineralized bone matrix, respectively. Deletion of the mTOR inhibitor tuberous sclerosis complex 1 (TSC1) in bone marrow mesenchymal stem cells (osteoblast precursors) results in thickened diaphyses due to increased peri- and endosteal bone matrix synthesis (Wu et al., 2017). Similarly, 40-60% of humans with an autosomal dominant genetic disease causing loss of function mutations in *TSC1* or *TSC2* display sclerotic bone lesions (Fang et al., 2015). Deletion of *TSC1* can induce similar phenotypes in mice, and treatment with Rap completely prevents the development of sclerotic lesions (Fang et al., 2015). Further, Rap treatment in young, skeletally immature rats decreased endochondral bone growth resulting in shorter diaphyses (Sanchez & He, 2009). Interestingly, Rap treatment increases osteoclastogenesis (Y. Zhang et al., 2017), while also increasing apoptosis and decreasing enzymatic activity in osteoclasts (Glantschnig, Fisher, Wesolowski, Rodan, & Reszka, 2003). These somewhat opposing responses in osteoclasts may act as a mechanism to protect against bone loss, as mTOR inhibition also decreases osteoblast differentiation and new bone matrix synthesis (Xian et al., 2012). If osteoclasts were able to develop unrestrained while osteoblast differentiation was blunted, there would be a stark loss of bone mass. Agreeing with this idea, rats treated with the mTOR-inhibitor everolimus displayed resistance to ovariectomy-induced bone loss (Kneissel et al., 2004) and Rap treatment attenuated age-related alveolar bone loss in mice (An et al., 2017).

Additionally, our findings show that a lower body weight with Rap and Rap+Met treatment is correlated to lower OA pathology and subchondral and diaphyseal bone thickness. This is in line with Wolff's law which states that bone will adapt to the forces to which it is subjected (J. Wolff,

1892). Therefore, the Rap-mediated decrease in bodyweight reduced loading forces within the joint space and along diaphysis, thus decreasing the stimulus for new bone matrix formation and reducing mechanical stress on the articular cartilage (Eric L Radin et al., 1984). Previous studies have demonstrated that lower bodyweight in calorie restricted animals results in lower OA pathology and femoral cortical thickness (Alison M. Bendele & Hulman, 1991; Hamrick et al., 2008; Radakovich et al., 2019). There is also precedent in the literature that dietary Rap (14ppm) treated male and female mice have lower bodyweight than control animals (Miller et al., 2011; Weiss et al., 2018). Therefore, to minimize the influence of dietary intake on treatment outcomes, we prorated food intake of the age-matched control animals to match the consumption of Rap and Rap+Met-treated animals. If caloric restriction were entirely responsible for the protective effects of Rap and Rap+Met, the same protection would have been observed in the control group. Caloric restriction in previous studies and Rap and Rap+Met treatment in the current study induce similar body weights in DH guinea pigs which indicates that smaller size may have partially contributed to the protective effects of Rap and Rap+Met. (Alison M. Bendele & Hulman, 1991; Hamrick et al., 2008; Radakovich et al., 2019). However, despite similar body weights after CR and Rap treatment in DH guinea pigs, the degree to which Rap and Rap+Met lowered OA scores in our study was greater than that of caloric restriction. While we cannot directly compare these two different studies, these findings may suggest that Rap and Rap+Met were exerting additional effects than weight restriction alone.

Although Rap and Rap+Met treatment were protective against primary OA and decreased subchondral cortical thickness, Met alone largely had no impact on OA pathology apart from preserving proteoglycan content. This differs from several studies in which Met has exerted chondroprotective effects in vitro (Petursson et al., 2013; C. Wang et al., 2018) or protected against

secondary OA in mice (Feng et al., 2020; Li et al., 2020) and rhesus monkeys (Li et al., 2020). In these studies, Met similarly prevented proteoglycan loss but also exerted additional effects to those observed in our study and was sufficient to decrease total OA score. Our study is unique in that we employed a primary model of OA. Our results could indicate that Met is one of the dichotomous treatments exerting differential effects on primary and secondary OA progression. However, retrospective analysis in humans showing diabetic patients receiving Met display decreased cartilage volume loss and lower incidence of knee replacement (Y. Wang et al., 2019) point to an alternative cause, most likely insufficient dose.

In our study, diet enriched with Met (1000ppm) resulted in an average consumption of 39.9±1.7 mg/kg/day and 44.5±5.7 mg/kg/day in DH guinea pigs treated with Met and Rap+Met, respectively. Assuming an average bodyweight of 70 kg, the highest approved Met dose for treatment of Type 2 Diabetes Mellitus in humans is 35 mg/kg/day (He & Wondisford, 2015), which is much lower than the doses at which Met has been shown to be protective against secondary OA by Feng et al. (2020; 200 mg/kg/day) and Li et al. (2020; 100, 200 mg/kg/day). However, the fractional bioavailability (F) of Met in circulation following oral consumption in rats (F=30%; Choi, Sang, & Lee, 2006) is lower than humans (F=55%; Graham et al., 2011), making a 100-300 mg/kg/day dose in rats clinically relevant. Therefore, the diet in our study may have provided a dose that is 6-7 fold lower than commonly observed in similarly sized rodents and humans. In support of this notion, Met concentrations ~2-3 hours after removing food from the cage were 277 ng/mL, which is 5-7-fold lower than the 1300-2000 ng/mL observed in healthy and diabetic humans following a normal therapeutic dose (Graham et al., 2011). Met is typically provided as a bolus 1-2 times per day and may also contribute to why the circulating concentration of Met would be lower in the current study where Met was provided ab libitum in the diet throughout the day.

Interestingly, the same dose that extended median lifespan and some indices of healthspan in the genetically homogenous C57BL/6 mice (Martin-Montalvo et al., 2013) showed no significant effect in genetically heterogenous UM-HET3 mice (Strong et al., 2016). Outbred animals like DH guinea pigs and UM-HET3 mice more closely recapitulate the diverse human population seen today. Therefore, if the dose of Met that benefits inbred animals is insufficient to benefit genetically heterogeneous animals, this may bring into question if Met can be translated to clinical populations as an anti-aging compound.

Despite providing novel findings, our study had some limitations and adverse effects. First, we have not yet directly measured mTOR activity in articular cartilage of DH guinea pigs. We anticipate completing immunohistochemical (IHC) analysis of articular cartilage to provide a more insight into mTOR activity, downstream targets, and the contribution to primary OA pathology. However, our data collectively show that Rap is able to inhibit mTOR in DH guinea pigs in periarticular muscle and in cultured chondrocytes. Rap or Rap+Met treatment in DH guinea pigs elevated blood glucose levels compared to controls. Hyperglycemia and impaired glucose tolerance are well documented side effects of Rap treatment (Miller et al., 2014; Weiss et al., 2018). The addition of Met to Rap treatment prevented the Rap-induced glucose intolerance in female but not male mice (Weiss et al., 2018). Similarly, Met treatment in the current study did not elicit a glucoregulatory protective effect in Rap treated male DH guinea pigs. We cannot specifically state that this was due to sex differences since we have not yet tested Rap and Rap+Met in female DH Guinea pigs and as stated previously the Met dose may have been too low. Treatment with Rap+Met also increased blood lactate concentrations compared to controls. Our unpublished data indicate that Rap and Rap+Met decreased maximal skeletal muscle oxidative capacity which may cause a compensatory increase in glycolytic flux and lactate production. To avoid the side

effects of systemic administration, treatment could have been injected intra-articularly to localize the effects of treatments to the joint space. However, Rap and Rap+Met are known for their ability to extend lifespan when consumed systemically. Therefore, administration via intra-articular injection would limit pleiotropic effects on tissues outside the joint space and likely unfasten the lifespan-extending properties of these compounds from their protective effects against OA pathology.

Our findings suggest that inhibition of the mTOR pathway is protective against primary OA pathology. Although our study was a necessary first step, we will next identify the mechanisms by which mTOR attenuation modifies primary, age-related OA. We acknowledge that a set of proximal mechanisms unique to primary and secondary OA initiate a cascade of homeostatic disturbances and may eventually converge on mutual pathways, such as mTOR, to elicit the same pathological hallmarks. However, the mechanisms downstream of mTOR may also differ, in which case mTOR is simply an overlapping node in two networks of dysregulation in pathways otherwise exclusive to primary and secondary OA. We are also interested in exploring different dosing intermittent dosing schemes or rapalogs with more specificity to inhibit mTOR and avoid unwanted side effects. Due to our likely insufficient dose of Met, further work is also needed to determine the utility of Met as a therapeutic agent against primary OA. Martin-Montalvo et al. (2013) showed that Met at the concentration provided in our study (1000 ppm) was sufficient to increase average lifespan in C57BL/6 mice, but became toxic and decreased lifespan at a dose 10-fold higher. Because of the mentioned differences in Met pharmacodynamics between rats and humans, it may be prudent to investigate the effects of Met on primary OA pathology using a dose in-between the extremes used by Martin-Montalvo et al. (2013).

CHAPTER 5: CONCLUSION

Extension of lifespan without a proportionate extension of healthspan could be considered detrimental. In our study, we show for the first time that the mTOR inhibitor Rap, alone or in combination with Met, can prevent the progression of age-related OA, the form of OA most commonly seen in aging humans. Rap and/or Rap+Met maintained articular cartilage structure, proteoglycan content and chondrocyte cellularity which culminated into lowering the total OA scores in the articular cartilage of the medial tibia. Met treatment alone preserved proteoglycan content but was not sufficient to lower the total OA score. In bone, Rap and Rap+Met decreased both subchondral and diaphyseal cortical thickness, suggesting that mTOR inhibition mediated a reduction in global cortical thickness rather than a site-specific resistance to subchondral sclerosis. These decreases in cortical thickness and cartilage OA scores were highly correlated to bodyweight, as is common in the DH guinea pig. However, Rap and Rap+Met seem to exert further benefits in articular cartilage compared to other studies in which caloric restriction reduced bodyweight and OA severity. Therefore, Rap delays the onset of OA by more than decreasing bodyweight alone. Met exerted no apparent effects on cortical bone and minimally affected articular cartilage, which was likely due to an insufficient dose and will require further investigation. Our findings reveal the pathological contribution of mTOR in primary OA and our future research aims to explore the down- and upstream mechanisms by which mTOR inhibition imparts resistance to age-related OA pathology.

CHAPTER 6: TABLE AND FIGURES

Average Daily Intake		Experimental Diet		
		Rapamycin (14 ppm)	Metformin (1000 ppm)	Rapamycin+Metformin (14 ppm, 1000 ppm)
Rapamycin	mg/day	0.61±0.07	-	0.54±0.06
	mg/kg/day	0.72±0.06	-	0.68±0.09
Metformin	mg/day	-	38.2±2.0	35.5±3.9
	mg/kg/day	-	39.9±1.7	44.5±5.7

Table 1. Average daily intake of Rap and Met for DH guinea pigs receiving experimental diets. All data are presented as mean ± SD.

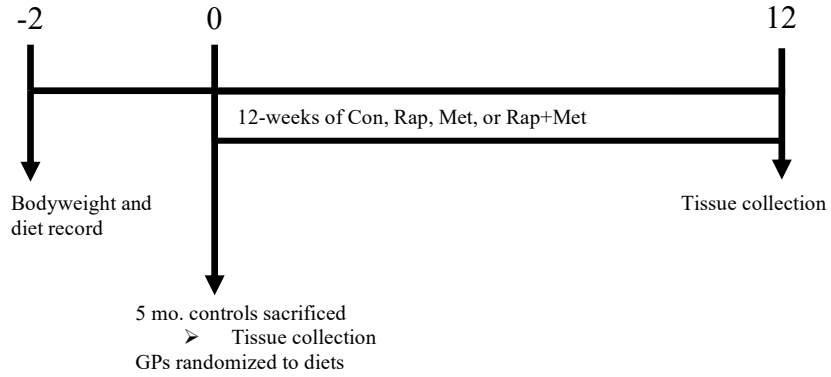

Figure 1: Schematic of experimental design.

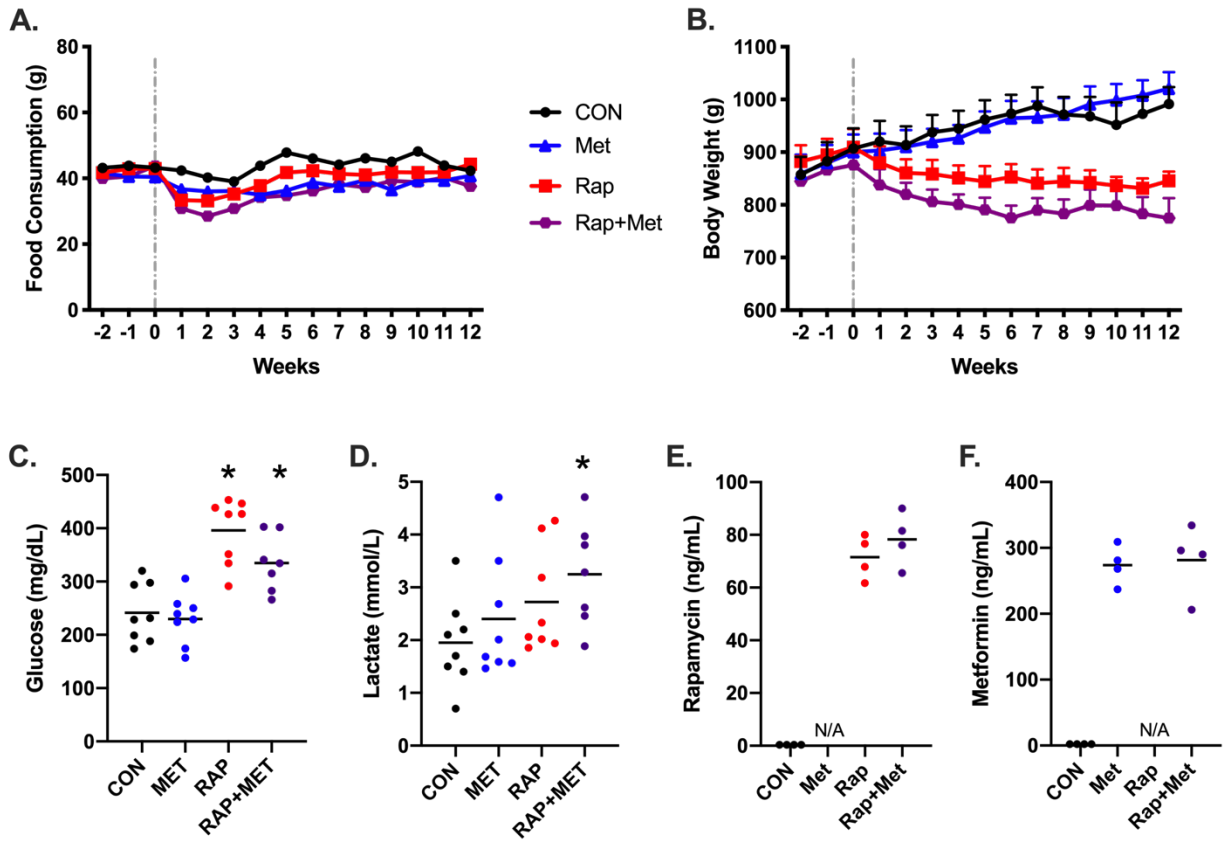

Figure 2: Effects of rapamycin, metformin and rapamycin+metformin in bodyweight, glucose and lactate metabolism, and circulating rapamycin and metformin. Average weekly (A) food consumption and (B) body weight of DH guinea pigs beginning 2 weeks prior to randomization and through the 12-weeks of treatment. Blood glucose (C), lactate (D), rapamycin (E) and metformin (F) collected at sacrifice.

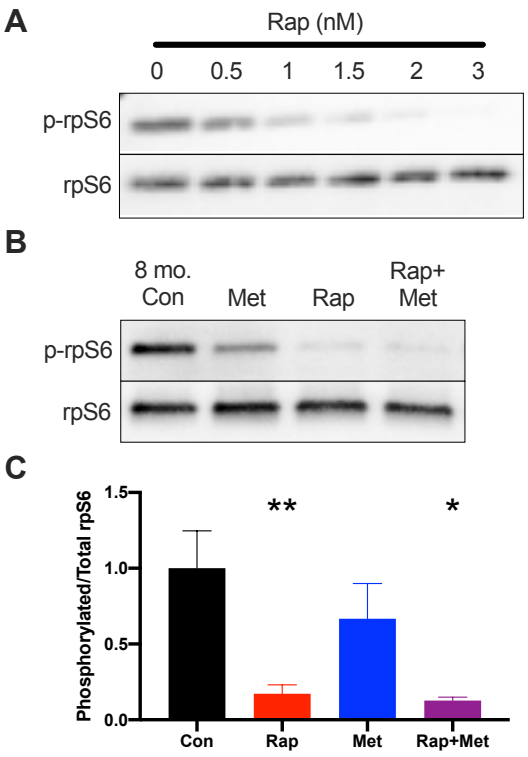

Figure 3: Rapamycin inhibits mTOR in articular chondrocytes and skeletal muscle.

A) Representative western blot images of phosphorylated- and total rpS6 from chondrocytes cultured in increasing concentrations of rapamycin for 48 hours (0 to 3nM) and (B) skeletal muscle of DH guinea pigs. C) Quantification of the ratio of phosphorylated to total rpS6. All data are expressed relative to 8 month controls. *$p<0.05$ vs 8 month control, **$p<0.01$ vs 8 month control).

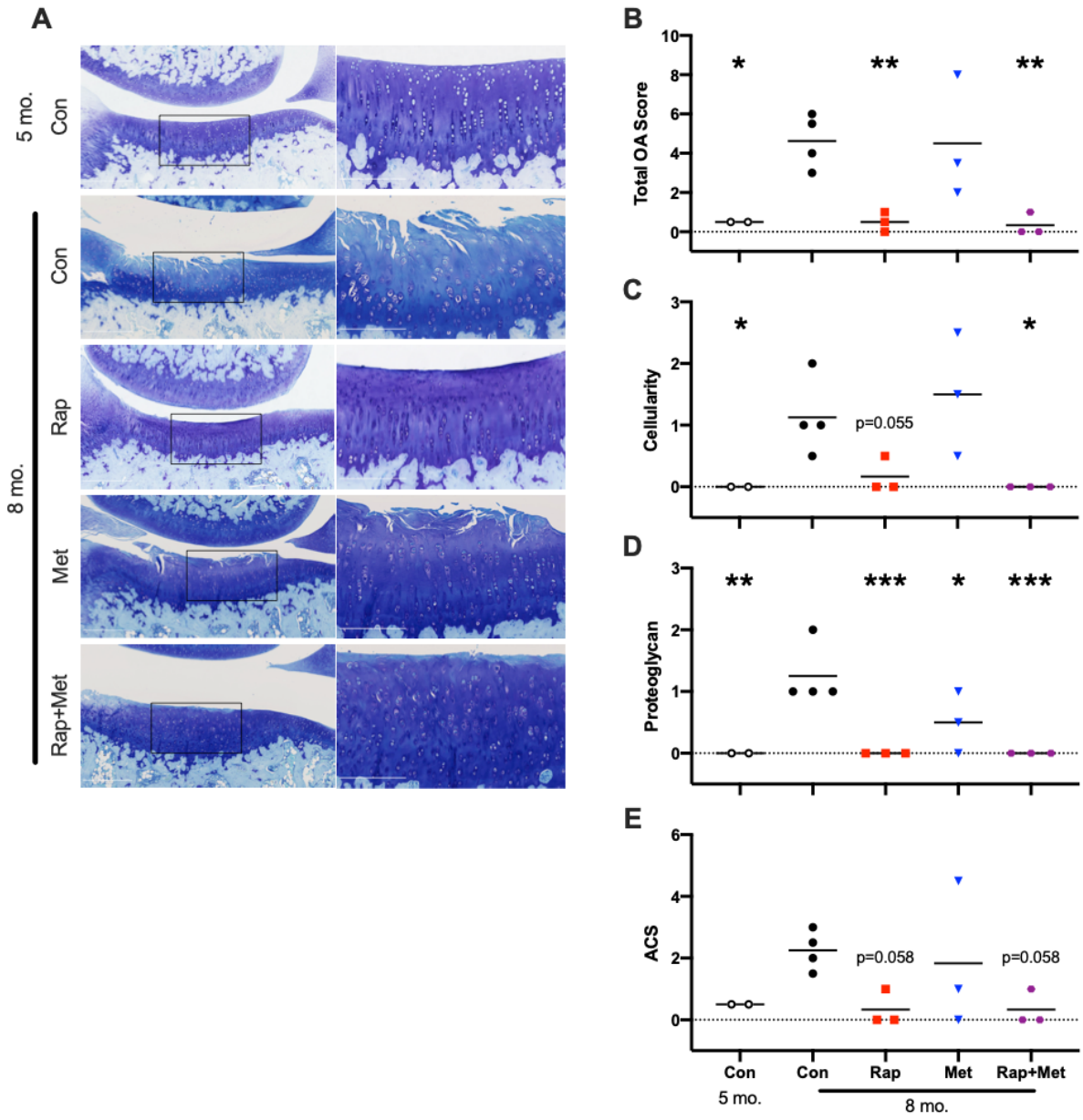

Figure 4: Rapamycin and rapamycin+metformin decreased OA pathology in medial tibial cartilage.

A) Toluidine blue staining of knee joint sections from 5-month control, 8-month control, and rapamycin, metformin, and rapamycin+metformin-treated DH guinea pigs. Rapamycin and rapamycin+metformin treatment resulted in lower total OARSI scores (B). Individual OARSI criteria including chondrocyte cellularity (C), proteoglycan content (D), and articular cartilage structure (ACS; E) are also shown. (*p<0.05 compared to 8 mo. controls; **p<0.01 compared to 8 mo. controls; ***p<0.001 compared to 8 mo. controls)

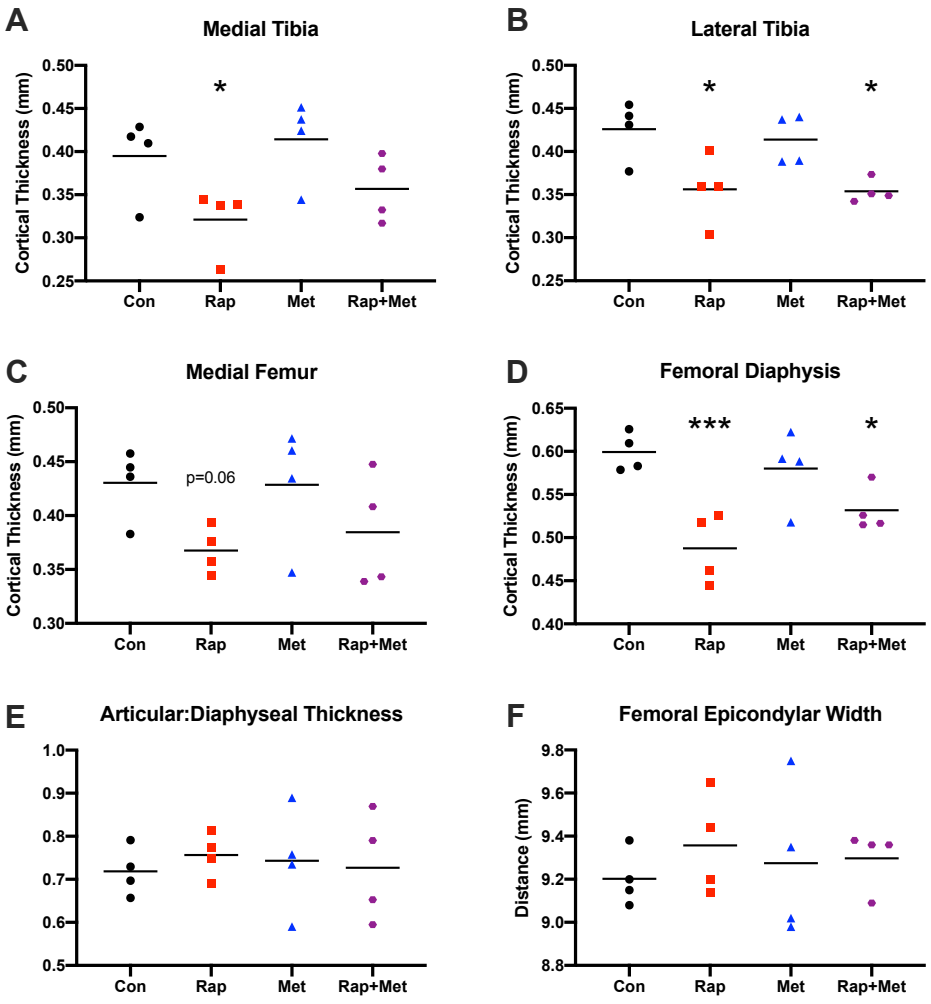

Figure 5: Rapamycin and rapamycin+metformin reduced articular cortical thickness.

Subchondral cortical thickness measured in the medial tibia (A), lateral tibia (B) medial femur (C), and femoral diaphysis (D). The ratio of articular to diaphyseal thickness (E) and femoral epicondylar width (F) were not different between groups. (*$p<0.05$ compared to control, ***$p<0.001$ compared to control)

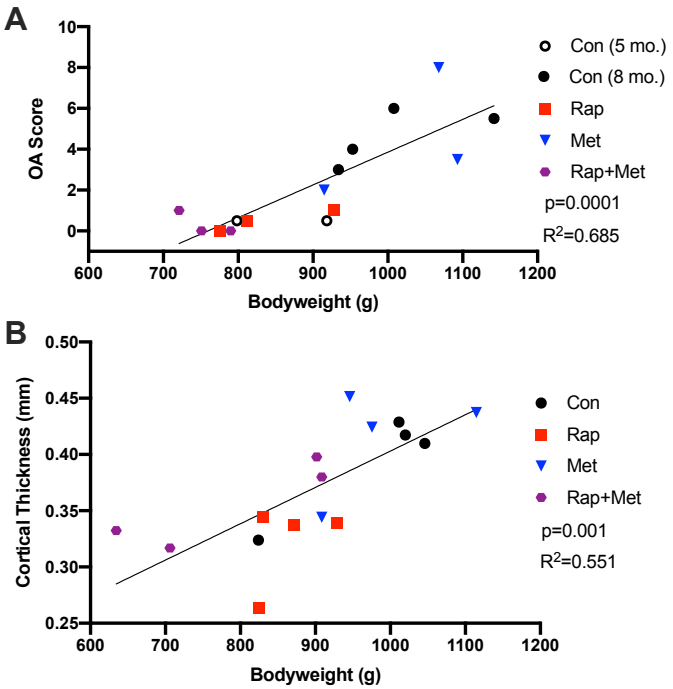

Figure 6: OA score and subchondral cortical thickness were correlated to bodyweight.

OA score (A; R^2=0.685, p=0.0001) and subchondral cortical thickness (B; R^2=0.551, p=0.001) displayed a significant positive correlation with bodyweight at sacrifice.

REFERENCES

Aki, T., Hashimoto, K., Ogasawara, M., & Itoi, E. (2018). A whole-genome transcriptome analysis of articular chondrocytes in secondary osteoarthritis of the hip. *PLoS ONE*, *13*(6), 1–17. https://doi.org/10.1371/journal.pone.0199734

An, J. Y., Quarles, E. K., Mekvanich, S., Kang, A., Liu, A., Santos, D., … Kaeberlein, M. (2017). Rapamycin treatment attenuates age-associated periodontitis in mice. *GeroScience*, *39*(4), 457–463. https://doi.org/10.1007/s11357-017-9994-6

Bendele, A. M., & Hulman, J. F. (1988). Spontaneous cartilage degeneration in guinea pigs. *Arthritis & Rheumatism*, *31*(4), 561–565. https://doi.org/10.1002/art.1780310416

Bendele, Alison M., & Hulman, J. F. (1991). Effects of body weight restriction on the development and progression of spontaneous osteoarthritis in guinea pigs. *Arthritis & Rheumatism*, *34*(9), 1180–1184. https://doi.org/10.1002/art.1780340916

Bohensky, J., Leshinsky, S., Srinivas, V., & Shapiro, I. M. (2010). Chondrocyte autophagy is stimulated by HIF-1 dependent AMPK activation and mTOR suppression. *Pediatric Nephrology*, *25*(4), 633–642. https://doi.org/10.1007/s00467-009-1310-y

Bouderlique, T., Vuppalapati, K. K., Newton, P. T., Li, L., Barenius, B., & Chagin, A. S. (2016). Targeted deletion of Atg5 in chondrocytes promotes age-related osteoarthritis. *Annals of the Rheumatic Diseases*, *75*(3), 627–631. https://doi.org/10.1136/annrheumdis-2015-207742

Brown, N. F., Stefanovic-Racic, M., Sipula, I. J., & Perdomo, G. (2007). The mammalian target of rapamycin regulates lipid metabolism in primary cultures of rat hepatocytes. *Metabolism: Clinical and Experimental*, *56*(11), 1500–1507. https://doi.org/10.1016/j.metabol.2007.06.016

Brown, T. D., Johnston, R. C., Saltzman, C. L., Marsh, J. L., & Buckwalter, J. A. (2006).

Posttraumatic osteoarthritis: A first estimate of incidence, prevalence, and burden of disease. *Journal of Orthopaedic Trauma*, *20*(10), 739–744. https://doi.org/10.1097/01.bot.0000246468.80635.ef

Buie, H. R., Campbell, G. M., Klinck, R. J., MacNeil, J. A., & Boyd, S. K. (2007). Automatic segmentation of cortical and trabecular compartments based on a dual threshold technique for in vivo micro-CT bone analysis. *Bone*, *41*(4), 505–515. https://doi.org/10.1016/j.bone.2007.07.007

Burr, D. B., & Gallant, M. A. (2012). Bone remodelling in osteoarthritis. *Nature Reviews Rheuematology*, *8*(11), 665–673. https://doi.org/10.1038/nrrheum.2012.130

Caramés, B., Hasegawa, A., Taniguchi, N., Miyaki, S., Blanco, F., & Lotz, M. (2012). Autophagy activation by rapamycin reduces severity of experimental osteoarthritis. *Annals of the Rheumatic Diseases*, *71*(4), 575–571. https://doi.org/10.1007/s00192-017-3435-z

Carlson, C. S., Loeser, R. F., Purser, C. B., Gardin, J. F., & Jerome, C. P. (2009). Osteoarthritis in cynomolgus macaques III: Effects of age, gender, and subchondral bone thickness on the severity of disease. *Journal of Bone and Mineral Research*, *11*(9), 1209–1217. https://doi.org/10.1002/jbmr.5650110904

Chen, Jianquan, & Long, F. (2018). MTOR signaling in skeletal development and disease. *Bone Research*, *6*(1). https://doi.org/10.1038/s41413-017-0004-5

Chen, Jie, Ou, Y., Li, Y., Hu, S., Shao, L. W., & Liu, Y. (2017). Metformin extends C. Elegans lifespan through lysosomal pathway. *ELife*, *6*, 1–17. https://doi.org/10.7554/eLife.31268

Choi, Y. H., Sang, K. G., & Lee, M. G. (2006). Dose-independent pharmacokinetics of metformin in rats: Hepatic and gastrointestinal first-pass effects. *Journal of Pharmaceutical Sciences*, *95*(11), 2543–2552. https://doi.org/10.1002/jps

Crema, M. D., Cibere, J., Sayre, E. C., Roemer, F. W., Wong, H., Thorne, A., … Guermazi, A. (2014). The relationship between subchondral sclerosis detected with MRI and cartilage loss in a cohort of subjects with knee pain: The knee osteoarthritis progression (KOAP) study. *Osteoarthritis and Cartilage*, *22*(4), 540–546. https://doi.org/10.1016/j.joca.2014.01.006

Demidenko, Z. N., & Blagosklonny, M. V. (2008). Growth stimulation leads to cellular senescence when the cell cycle is blocked. *Cell Cycle*, *7*(21), 3355–3361. https://doi.org/10.4161/cc.7.21.6919

Doube, M., Klosowski, M. M., Arganda-Carreras, I., Cordelières, F. P., Dougherty, R. P., Jackson, J. S., … Shefelbine, S. J. (2010). BoneJ: Free and extensible bone image analysis in ImageJ. *Bone*, *47*(6), 1076–1079. https://doi.org/10.1016/j.bone.2010.08.023

Fang, F., Sun, S., Wang, L., Guan, J. L., Giovannini, M., Zhu, Y., & Liu, F. (2015). Neural crest-specific TSC1 deletion in mice leads to sclerotic craniofacial lesion. *Journal of Bone and Mineral Research*, *30*(7), 1195–1205. https://doi.org/10.1002/jbmr.2447

Feng, X., Pan, J., Li, J., Zeng, C., Qi, W., Shao, Y., … Cai, D. (2020). Metformin attenuates cartilage degeneration in an experimental osteoarthritis model by regulating AMPK / mTOR. *Aging*, *12*.

Fuerst, M., Bertrand, J., Lammers, L., Dreier, R., Echtermeyer, F., Nitschke, Y., … Rüther, W. (2009). Calcification of articular cartilage in human osteoarthritis. *Arthritis and Rheumatism*, *60*(9), 2694–2703. https://doi.org/10.1002/art.24774

Glantschnig, H., Fisher, J. E., Wesolowski, G., Rodan, G. A., & Reszka, A. A. (2003). M-CSF, TNFα and RANK ligand promote osteoclast survival by signaling through mTOR/S6 kinase. *Cell Death and Differentiation*, *10*(10), 1165–1177.

https://doi.org/10.1038/sj.cdd.4401285

Glasson, S. S., Chambers, M. G., Van Den Berg, W. B., & Little, C. B. (2010). The OARSI histopathology initiative - recommendations for histological assessments of osteoarthritis in the mouse. *Osteoarthritis and Cartilage*, *18*(SUPPL. 3), S17–S23. https://doi.org/10.1016/j.joca.2010.05.025

Graham, G. G., Punt, J., Arora, M., Day, R. O., Doogue, M. P., Duong, J. K., … Williams, K. M. (2011). Clinical pharmacokinetics of metformin. *Clinical Pharmacokinetics*, *50*(2), 81–98. https://doi.org/10.2165/11534750-000000000-00000

Hamrick, M. W., Ding, K. H., Ponnala, S., Ferrari, S. L., & Isales, C. M. (2008). Caloric restriction decreases cortical bone mass but spares trabecular bone in the mouse skeleton: Implications for the regulation of bone mass by body weight. *Journal of Bone and Mineral Research*, *23*(6), 870–878. https://doi.org/10.1359/jbmr.080213

Hardie, D. G., Ross, F. A., & Hawley, S. A. (2012). AMPK - a nutrient and energy sensor that maintains energy homeostasis. *Nature Reviews Molecular Cell Biology*, *13*(4), 251–262. https://doi.org/10.1038/nrm3311.AMPK

Harrison, D. E., Strong, R., Sharp, Z. D., Nelson, J. F., Astle, C. M., Flurkey, K., … Miller, R. A. (2009). Rapamycin fed late in life extends lifespan in genetically heterogeneous mice. *Nature*, *460*(7253), 392–395. https://doi.org/10.1038/nature08221

Hawley, S. A., Gadalla, A. E., Olsen, G. S., & Hardie, D. G. (2002). The antidiabetic drug metformin activates the AMP-activated protein kinase cascade via an adenine nucleotide-independent mechanism. *Cell*, *51*(August).

He, L., & Wondisford, F. E. (2015). Metformin action: Concentrations matter. *Cell Metabolism*, *21*(2), 159–162. https://doi.org/10.1016/j.cmet.2015.01.003

Houde, V. P., Brûlé, S., Festuccia, W. T., Blanchard, P. G., Bellmann, K., Deshaies, Y., & Marette, A. (2010). Chronic rapamycin treatment causes glucose intolerance and hyperlipidemia by upregulating hepatic gluconeogenesis and impairing lipid deposition in adipose tissue. *Diabetes*, *59*(6), 1338–1348. https://doi.org/10.2337/db09-1324

Huebner, J. L., Hanes, M. A., Beekman, B., TeKoppele, J. M., & Kraus, V. B. (2002). A comparative analysis of bone and cartilage metabolism in two strains of guinea-pig with varying degrees of naturally occurring osteoarthritis. *Osteoarthritis and Cartilage*, *10*(10), 758–767. https://doi.org/10.1053/joca.2002.0821

Huebner, J. L., & Kraus, V. B. (2006). Assessment of the utility of biomarkers of osteoarthritis in the guinea pig. *Osteoarthritis and Cartilage*, *14*(9), 923–930. https://doi.org/10.1016/j.joca.2006.03.007

Johnson, S. C., Rabinovich, P. S., & Kaeberlin, M. (2013). mTOR is a key modulator of ageing and age-related disease. *Nature*, *493*(7432), 338–345. https://doi.org/10.1038/nature11861.mTOR

Kaeberlein, M., Powers, R. W., Steffen, K. K., Westman, E. A., Hu, D., Dang, N., … Kennedy, B. K. (2005). Regulation of yeast replicative life span by TOR and Sch9 response to nutrients. *Science*, *310*(5751), 1193–1196. https://doi.org/10.1126/science.1115535

Kapadia, R. D., Badger, A. M., Levin, J. M., Swift, B., Bhattacharyya, A., Dodds, R. A., … Lark, M. W. (2000). Meniscal ossification in spontaneous osteoarthritis in the guinea-pig. *Osteoarthritis and Cartilage*, *8*(5), 374–377. https://doi.org/10.1053/joca.1999.0312

Kennedy, B. K., Berger, S. L., Brunet, A., Campisi, J., Cuervo, A. M., Epel, E. S., … Sierra, F. (2014). Aging: a common driver of chronic diseases and a target for novel interventions. *Cell*, *159*(4), 709–713. https://doi.org/10.1016/j.cell.2014.10.039

Kneissel, M., Luong-Nguyen, N. H., Baptist, M., Cortesi, R., Zumstein-Mecker, S., Kossida, S., … Susa, M. (2004). Everolimus suppresses cancellous bone loss, bone resorption, and cathepsin K expression by osteoclasts. *Bone*, *35*(5), 1144–1156. https://doi.org/10.1016/j.bone.2004.07.013

Kraus, V. B., Huebner, J. L., DeGroot, J., & Bendele, A. (2010). The OARSI histopathology initiative - recommendations for histological assessments of osteoarthritis in the guinea pig. *Osteoarthritis and Cartilage*, *18*(SUPPL. 3), S35–S52. https://doi.org/10.1016/j.joca.2010.04.015

Li, J., Zhang, B., Liu, W. X., Lu, K., Pan, H., Wang, T., … Chen, D. (2020). Metformin limits osteoarthritis development and progression through activation of ampk signalling. *Annals of the Rheumatic Diseases*, 1–11. https://doi.org/10.1136/annrheumdis-2019-216713

Loeser, R. F., Goldring, S. R., Scanzello, C. R., & Goldring, M. B. (2012). Osteoarthritis: A disease of the joint as an organ. *Arthritis and Rheumatism*, *64*(6), 1697–1707. https://doi.org/10.1002/art.34453

Loeser, R., Kelley, K., Harper, L., & Carlson, C. (2018). Osteoarthritis severity in mice with deletions of JNK1 and JNK2: no protection after DMM surgery and enhancement of age-related OA with JNK2 deletion. *Osteoarthritis and Cartilage*, *26*(2018), S31. https://doi.org/10.1016/j.joca.2018.02.078

Loewith, R., & Hall, M. N. (2011). Target of rapamycin (TOR) in nutrient signaling and growth control. *Genetics*, *189*(4), 1177–1201. https://doi.org/10.1534/genetics.111.133363

Martin-Montalvo, A., Mercken, E. M., Mitchell, S. J., Palacios, H. H., Mote, P. L., Scheibye-Knudsen, M., … De Cabo, R. (2013). Metformin improves healthspan and lifespan in mice. *Nature Communications*, *4*. https://doi.org/10.1038/ncomms3192

Miller, R. A., Harrison, D. E., Astle, C. M., Baur, J. A., Boyd, A. R., De Cabo, R., … Strong, R. (2011). Rapamycin, but not resveratrol or simvastatin, extends life span of genetically heterogeneous mice. *Journals of Gerontology - Series A Biological Sciences and Medical Sciences*, *66 A*(2), 191–201. https://doi.org/10.1093/gerona/glq178

Miller, R. A., Harrison, D. E., Astle, C. M., Fernandez, E., Flurkey, K., Han, M., … Strong, R. (2014). Rapamycin-mediated lifespan increase in mice is dose and sex dependent and metabolically distinct from dietary restriction. *Aging Cell*, *13*(3), 468–477. https://doi.org/10.1111/acel.12194

Moon, P. M., Shao, Z., Penuela, S., Laird, D. W., & Beier, F. (2018). Opposite roles of pannexins in post-traumatic versus aging associated osteoarthritis. *Osteoarthritis and Cartilage*, *26*(2018), S115. https://doi.org/10.1016/j.joca.2018.02.250

Murphy, L. B., Cisternas, M. G., Pasta, D. J., Helmick, C. G., & Yelin, E. H. (2018). Medical expenditures and earnings losses among US adults with arthritis in 2013. *Arthritis Care and Research*, *70*(6), 869–876. https://doi.org/10.1002/acr.23425

Murray, C. J. L., Abraham, J., Ali, M. K., Alvarado, M., Atkinson, C., Baddour, L. M., … Zabetian, A. (2013). The State of US health, 1990-2010: Burden of diseases, injuries, and risk factors. *JAMA - Journal of the American Medical Association*, *310*(6), 591–608. https://doi.org/10.1001/jama.2013.13805

Nadon, N. L., Strong, R., Miller, R. A., Nelson, J., Javors, M., Sharp, Z. D., … Harrison, D. E. (2008). Design of aging intervention studies: The NIA interventions testing program. *Age*, *30*(4), 187–199. https://doi.org/10.1007/s11357-008-9048-1

Neogi, T., & Zhang, Y. (2013). Epidemiology of OA. *Rheumatic Diseases Clinincs of North America*, *39*(1), 1–19. https://doi.org/10.1016/j.rdc.2012.10.004.Epidemiology

O'Conor, C. J., Ramalingam, S., Zelenski, N. A., Benefield, H. C., Rigo, I., Little, D., … Guilak, F. (2016). Cartilage-specific knockout of the mechanosensory ion channel TRPV4 decreases age-related osteoarthritis. *Scientific Reports*, *6*(July), 1–10. https://doi.org/10.1038/srep29053

Owen, M. R., Doran, E., & Halestrap, A. P. (2000). Evidence that metformin exerts its anti-diabetic effects through inhibition of complex 1 of the mitochondrial respiratory chain. *Biochemical Journal*, *348*(3), 607–614. https://doi.org/10.1042/bj3480607

Pal, B., Endisha, H., Zhang, Y., & Kapoor, M. (2015). mTOR: A potential therapeutic target in osteoarthritis? *Drugs in R and D*, *15*(1), 27–36. https://doi.org/10.1007/s40268-015-0082-z

Petursson, F., Terkeltaub, R., Liu-Bryan, R., Husa, M., June, R., & Lotz, M. (2013). Linked decreases in liver kinase B1 and AMP-activated protein kinase activity modulate matrix catabolic responses to biomechanical injury in chondrocytes. *Arthritis Research and Therapy*, *15*(4), 1–11. https://doi.org/10.1186/ar4254

Philp, A., Schenk, S., Perez-Schindler, J., Hamilton, D. L., Breen, L., Laverone, E., … Baar, K. (2015). Rapamycin does not prevent increases in myofibrillar or mitochondrial protein synthesis following endurance exercise. *Journal of Physiology*, *593*(18), 4275–4284. https://doi.org/10.1113/JP271219

Radakovich, L. B., Marolf, A. J., Culver, L. A., & Santangelo, K. S. (2019). Calorie restriction with regular chow, but not a high-fat diet, delays onset of spontaneous osteoarthritis in the Hartley guinea pig model. *Arthritis Research and Therapy*, *21*(1), 1–14. https://doi.org/10.1186/s13075-019-1925-8

Radakovich, L. B., Marolf, A. J., Shannon, J. P., Pannone, S. C., Sherk, V. D., & Santangelo, K. S. (2018). Development of a microcomputed tomography scoring system to characterize

disease progression in the Hartley guinea pig model of spontaneous osteoarthritis. *Connective Tissue Research*, *59*(6), 523–533. https://doi.org/10.1080/03008207.2017.1409218

Radin, E. L., & Rose, R. M. (1986). Role of subchondral bone in the initiation and progression of cartilage damage. *Clinical Orthopaedics and Related Research*, *213*, 34–40.

Radin, Eric L, Martin, R. B., Burr, D. B., Caterson, B., Boyd, R. D., & Goodwin, C. (1984). Effects of mechanical loading on the tissues of the rabbit knee. *Journal of Orthopaedic Research*, *2*, 221–234.

Reznick, R. M., Zong, H., Li, J., Morino, K., Moore, I. K., Yu, H. J., … Shulman, G. I. (2007). Aging-associated reductions in AMP-activated protein kinase activity and mitochondrial biogenesis. *Cell Metabolism*, *5*(2), 151–156. https://doi.org/10.1016/j.cmet.2007.01.008

Roh, C., Han, J., Tzatsos, A., & Kandror, K. V. (2003). Nutrient-sensing mTOR-mediated pathway regulates leptin production in isolated rat adipocytes. *American Journal of Physiology - Endocrinology and Metabolism*, *284*(2 47-2), 322–330. https://doi.org/10.1152/ajpendo.00230.2002

Rothwell, A. G., & Bentley, G. (1973). Chondrocyte multiplication in osteoarthritic articular cartilage. *Journal of Bone and Joint Surgery - Series B*, *55*(3), 588–594. https://doi.org/10.1302/0301-620X.55B3.588

Sabers, C. J., Martin, M. M., Brunn, G. J., Williams, J. M., Dumont, F. J., Wiederrecht, G., & Abraham, R. T. (1995). Isolation of a protein target of the FKBP12-rapamycin complex in mamalian cells. *The Journal of Biological Chemistry*.

Salminen, A., & Kaarniranta, K. (2012). AMP-activated protein kinase (AMPK) controls the aging process via an integrated signaling network. *Ageing Research Reviews*, *11*(2), 230–

241. https://doi.org/10.1016/j.arr.2011.12.005

Sanchez, C. P., & He, Y. Z. (2009). Bone growth during rapamycin therapy in young rats. *BMC Pediatrics*, *9*, 3. https://doi.org/10.1186/1471-2431-9-3

Sasaki, H., Takayama, K., Matsushita, T., Ishida, K., Kubo, S., Matsumoto, T., … Kuroda, R. (2012). Autophagy modulates osteoarthritis-related gene expression in human chondrocytes. *Arthritis and Rheumatism*, *64*(6), 1920–1928. https://doi.org/10.1002/art.34323

Schneider, C., Rasband, W., & Eliceiri, K. (2012). NIH Image to ImageJ: 25 years of image analysis. *Nature Methods*, *9*(7), 671–675.

Stockwell, R. A. (1991). Cartilage failure in osteoarthritis: Relevance of normal structure and function. A review. *Clinical Anatomy*, *4*(3), 161–191. https://doi.org/10.1002/ca.980040303

Strong, R., Miller, R. A., Antebi, A., Astle, C. M., Bogue, M., Denzel, M. S., … Harrison, D. E. (2016). Longer lifespan in male mice treated with a weakly estrogenic agonist, an antioxidant, an α-glucosidase inhibitor or a Nrf2-inducer. *Aging Cell*, *15*(5), 872–884. https://doi.org/10.1111/acel.12496

Sun, Y., & Mauerhan, D. R. (2012). Meniscal calcification, pathogenesis and implications. *Current Opinion in Rheumatology*, *24*(2), 152–157. https://doi.org/10.1097/BOR.0b013e32834e90c1

Takayama, K., Kawakami, Y., Kobayashi, M., Greco, N., Cummins, J. H., Matsushita, T., … Huard, J. (2014). Local intra-articular injection of rapamycin delays articular cartilage degeneration in a murine model of osteoarthritis. *Arthritis Research and Therapy*, *16*(1), 1–10. https://doi.org/10.1186/s13075-014-0482-4

Tardif, S., Ross, C., Bergman, P., Fernandez, E., Javors, M., Salmon, A., … Richardson, A. (2015). Testing efficacy of administration of the antiaging drug rapamycin in a nonhuman

primate, the common marmoset. *Journals of Gerontology - Series A Biological Sciences and Medical Sciences*, *70*(5), 577–588. https://doi.org/10.1093/gerona/glu101

Terkeltaub, R., Yang, B., Lotz, M., & Liu-Bryan, R. (2011). Chondrocyte AMP-activated protein kinase activity suppresses matrix degradation responses to proinflammatory cytokines interleukin-1β and tumor necrosis factor α. *Arthritis and Rheumatism*, *63*(7), 1928–1937. https://doi.org/10.1002/art.30333

Usmani, S. E., Ulici, V., Pest, M. A., Hill, T. L., Welch, I. D., & Beier, F. (2016). Context-specific protection of TGFα null mice from osteoarthritis. *Scientific Reports*, *6*(July), 1–11. https://doi.org/10.1038/srep30434

Vellai, T., Takacs-Vellai, K., Zhang, Y., Kovacs, A. L., Orosz, L., & Müller, F. (2003). Influence of TOR kinase on lifespan in C. elegans. *Nature*, *426*(6967), 620. https://doi.org/10.1038/426620a

Wang, C., Yang, Y., Zhang, Y., Liu, J., Yao, Z., & Zhang, C. (2018). Protective effects of metformin against osteoarthritis through upregulation of SIRT3-mediated PINK1/Parkin-dependent mitophagy in primary chondrocytes. *BioScience Trends*, *12*(6), 605–612. https://doi.org/10.5582/bst.2018.01263

Wang, T., Wen, C. Y., Yan, C. H., Lu, W. W., & Chiu, K. Y. (2013). Spatial and temporal changes of subchondral bone proceed to microscopic articular cartilage degeneration in guinea pigs with spontaneous osteoarthritis. *Osteoarthritis and Cartilage*, *21*(4), 574–581. https://doi.org/10.1016/j.joca.2013.01.002

Wang, Y., Hussain, S. M., Wluka, A. E., Lim, Y. Z., Abram, F., Pelletier, J. P., … Cicuttini, F. M. (2019). Association between metformin use and disease progression in obese people with knee osteoarthritis: Data from the Osteoarthritis Initiative - A prospective cohort study.

Arthritis Research and Therapy, *21*(1), 1–6. https://doi.org/10.1186/s13075-019-1915-x

Weiss, R., Fernandez, E., Liu, Y., Strong, R., & Salmon, A. B. (2018). Metformin reduces glucose intolerance caused by rapamycin treatment in genetically heterogeneous female mice. *Aging*, *10*(3), 386–401. https://doi.org/10.18632/aging.101401

Woessner, J. F., & Gunja-Smith, Z. (1991). Role of metalloproteinases in human osteoarthritis. *The Journal of Rheumatology, Supplement*, *27*, 99–101.

Wolff, C. A., Reid, J. J., Musci, R. V., Linden, M. A., Konopka, A. R., Peelor, F. F., … Hamilton, K. L. (2020). Differential effects of rapamycin and metformin in combination with rapamycin on mechanisms of proteostasis in cultured skeletal myotubes. *Journals of Gerontology - Series A Biological Sciences and Medical Sciences*, *75*(1), 32–39. https://doi.org/10.1093/gerona/glz058

Wolff, J. (1892). Das Gesetz der Transformation der Knochen. *Springer, Berlin*.

Wu, H., Wu, Z., Li, P., Cong, Q., Chen, R., Xu, W., … Li, B. (2017). Bone size and quality regulation: Concerted actions of mTOR in mesenchymal stromal cells and osteoclasts. *Stem Cell Reports*, *8*(6), 1600–1616. https://doi.org/10.1016/j.stemcr.2017.04.005

Xian, L., Wu, X., Pang, L., Lou, M., Rosen, C., Qui, T., … Cao, X. (2012). Matrix IGF-1 regulates bone mass by activation of mTOR in mesenchymal stem cells. *Nature Medicine*, *18*(7), 1095–1101. https://doi.org/10.1038/nm.2793.Matrix

Yu, D., Hu, J., Sheng, Z., Fu, G., Wang, Y., Chen, Y., … Ouyang, H. (2020). Dual roles of misshapen/NIK-related kinase (MINK1) in osteoarthritis subtypes through the activation of TGFβ signaling. *Osteoarthritis and Cartilage*, *28*(1), 112–121. https://doi.org/10.1016/j.joca.2019.09.009

Zhang, H., Wang, H., Zeng, C., Yan, B., Ouyang, J., Liu, X., … Cai, D. (2017). mTORC1

activation downregulates FGFR3 and PTH/PTHrP receptor in articular chondrocytes to initiate osteoarthritis. *Osteoarthritis and Cartilage*, *25*(6), 952–963. https://doi.org/10.1016/j.joca.2016.12.024

Zhang, Y., Vasheghani, F., Li, Y. H., Blati, M., Simeone, K., Fahmi, H., … Kapoor, M. (2015). Cartilage-specific deletion of mTOR upregulates autophagy and protects mice from osteoarthritis. *Annals of the Rheumatic Diseases*, *74*(7), 1432–1440. https://doi.org/10.1136/annrheumdis-2013-204599

Zhang, Y., Xu, S., Li, K., Tan, K., Liang, K., Wang, J., … Bai, X. (2017). mTORC1 inhibits NF-κB/NFATc1 signaling and prevents osteoclast precursor differentiation, In vitro and In mice. *Journal of Bone and Mineral Research*, *32*(9), 1829–1840. https://doi.org/10.1002/jbmr.3172

Zhou, S., Lu, W., Chen, L., Ge, Q., Chen, D., Xu, Z., … Jiang, Q. (2017). AMPK deficiency in chondrocytes accelerated the progression of instability-induced and ageing-associated osteoarthritis in adult mice. *Scientific Reports*, *7*(1), 1–14. https://doi.org/10.1038/srep43245

Zuck, T. T. (1938). Age order of epiphyseal union in the guinea pig. *The Anatomical Record*, *70*(4), 389–399.